

The Mount Cameroon Volcano, West Africa: an active link between recent eruptives and mantle signatures of the deep past beneath the margins of Africa

M.S. Njome^{1,2}, C.E. Suh² and M.J. de Wit¹

1. Africa Earth Observatory Network (AEON), Geological Sciences Extension Building, Ring Road, University of Cape Town, Private Bag X3 Rondebosch, 7701, South Africa. E-mails: njome.stephen@uct.ac.za; Maarten.DeWit@uct.ac.za
2. Department of Geology and Environmental Science, University of Buea, P.O. Box 63, Buea, South West Region, Cameroon. (E-mails: mnjome@yahoo.com; chuhma@yahoo.com)

ABSTRACT

Mount Cameroon, a 4095 m high stratovolcano is arguably the most active volcano in Equatorial West Africa, with seven eruptions during the last century. It is the only active member of the 1600 km long volcanic belt – “Cameroon Volcanic Line (CVL)” - with a history going back ~ 80 Ma at the initial opening of the Central Atlantic Ocean during the Cretaceous. In order to decipher recent petrogenetic and geotectonic evolution of the CVL at this volcano, Lava samples of unknown ages but older than all 20th century lavas are investigated for their mineral chemistry and whole rock geochemistry and compared with the 20th century lavas that have been the only focus of petrological investigations for the past three decades.

The data show all lavas as within plate and lava types (basalt, basanite/trachy-basalt, hawaiite and basaltic trachy-andesite) indicating these historical eruptions involved even more evolved magmas than those of the 20th century. The lavas are nepheline normative and show an alkaline affinity associated with rift-graben structures, fed from fissures and central vents.

Most samples are olivine, clinopyroxene and plagioclase feldspar phyric with additional Fe-Ti oxide phenocrysts. Mineral chemistry data show the compositional range of olivine for older lava samples to be very wide (Fo_{58%-84%}) and a broader plagioclase composition extending to intermediate andesine, a composition which has not been reported for any 20th century lavas.

Despite these differences, primitive mantle normalized trace element spidergrams show similar pattern for these older lavas as the 20th century lavas, similar to OIB, confirming they all have a common mantle source of HIMU type. Thus, whilst the precise origin of the CVL is still disputed, it is clear that its mantle source area is not a transient plume. This has major implications for understanding mantle processes marginal to evolving passive Atlantic margins.

Key words: Mount Cameroon; 20th Century lavas; older lavas; evolved magmas; common mantle source.

INTRODUCTION

Mount Cameroon (04° 13' N, 09° 10' E), a 4095 m high stratovolcano adorning the Gulf of Guinea is West Africa's most active volcano with 7 eruptions during the last century. It is also the only active member of the 1600 km long NE - SW alignment of volcanoes - Cameroon Volcanic Line (CVL)(**Figure 1**) - interpreted

to follow a Precambrian palaeo-shear zone (Central African Shear Zone-CASZ), a pre-Mesozoic drift extension of the Pernambuco Shear Zone in NE Brazil (Archanjo et al., 2002; Ngako et al., 2003). Thus, Mount Cameroon cannot be regarded only as a volcano, but as a volcano-tectonic feature. Its unique geotectonic position at the African Continent – Atlantic Ocean

boundary is of vital importance in understanding the geodynamic assembly of West Gondwana.

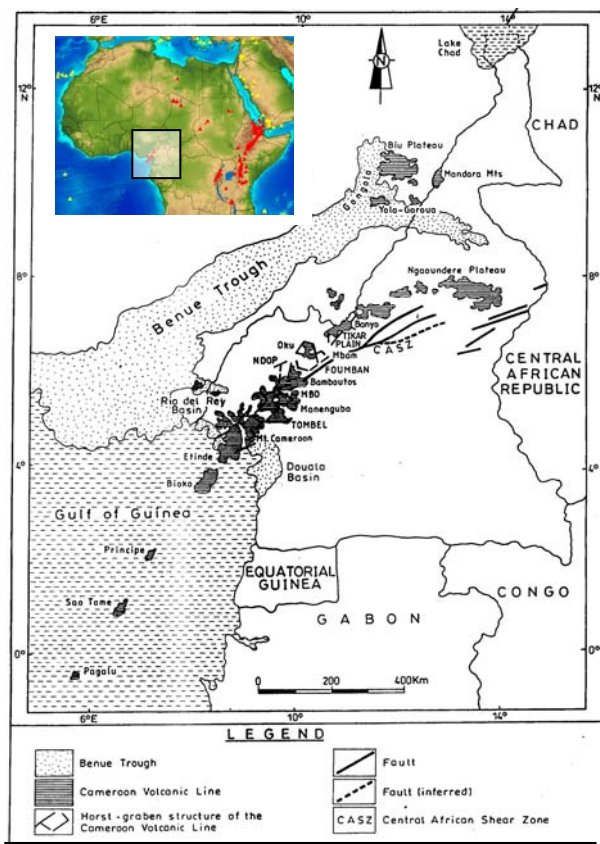


Figure 1.: Map showing the Cameroon Volcanic Line and related adjacent Cretaceous sedimentary rocks of the Benue trough all dividing into two branches at the northern ends. The Central African Shear Zone (CASZ) (thick fault lines) and the horst (lowercase letters) – graben (uppercase letters) structure (thinner fault lines) of the southern part of the line are shown. (Modified from Fitton and Dunlop, 1985 and Deruelle et al., 1987). Insert: CVL in rectangular box (Global Volcanism Program, <http://www.volcano.si.edu/world/region.cfm?num=02>)

Volcanological and petrochemical investigations at this volcano have largely been limited to Recent lavas of known ages (e.g., Fitton et al., 1983; Deruelle et al., 2000; Suh et al., 2003; Suh et al., 2008; Njome et al., 2008) despite the fact that the whole massif is a great pile of basalts and pyroclastics. In this study, lava samples of unknown ages, but clearly older than all the 20th century lavas were subjected under petrographical, mineral and whole rock geochemical investigations which have been used for the younger samples in a bid to decipher any petrochemical evolutionary trends and expand understanding of magma origin and plumbing beneath this volcano.

METHOD AND RESULTS

Petrography

Thin sections were prepared from rock samples collected and investigated under a petrographic microscope for their mineralogical proportions and textures. The relative proportions of the different mineral phases were determined using an automatic point counter. Petrographic examination of 26 samples of the older lavas show that just like the younger samples, most are olivine, clinopyroxene and plagioclase feldspar phyrlic with additional Fe-Ti oxide phenocrysts. Point-counted modal analyses for representative samples (**Table 1**) show most 20th century lavas having all major phenocryst phases while the older lavas show a lot of variations in their phenocryst content (depending on the degree of crystallinity).

Clinopyroxene is the dominant phenocryst phase of all younger lavas and in moderately-to coarse-porphyrific samples of the older lavas (**Table 1**); often as the largest phenocrysts (0.6 mm - 5.8 mm). Most commonly they occur as crystal aggregates (glomeroporphyritic texture) though a large number also occur as single individual large euhedral–subhedral crystals, typically twinned and well zoned (**Figure 2a**). Plagioclase feldspars are the next dominant phenocryst phase to clinopyroxene in the younger samples and in moderately porphyritic samples of the older flows and as the most dominant phenocryst phase in the sparsely-porphyrific samples of the older flows though occurring often as the smallest crystals (0.35 mm to 2.4 mm). They are typically twinned (showing both simple and polysynthetic twinning) and zoned (**Figure 2b**). Olivine occurs as large crystals (0.5 mm - 2.8 mm) and is the least abundant phenocryst phase. In older samples, it is next in dominance to clinopyroxene in the coarse-porphyrific samples (1.2 – 8.2 vol %); and occurs as the only phenocryst phase in aphyric samples. Generally, the larger crystals are often subhedral – euhedral in form, a large number showing resorption at their margins (**Figure 2c**). The groundmass is generally microlite-rich (>75 vol. %, but for the 1954 sample), made up of same minerals observed as phenocrysts, with plagioclase laths and microlites dominating over other phases (**Figure 2d**).

Mineral Chemistry

Representative microprobe analyses of phenocryst cores, rims and groundmass microlites for different lava samples are given in **Table 2**. Generally, all samples show olivine cores being richer in magnesium (Fo₇₇ – Fo₈₅) than the rims (Fo₆₉ – Fo₇₈). For younger samples, Microlites are more iron-rich (Fo₇₅ – Fo₆₉) than the phenocrysts (Fo₈₀ – Fo₇₇), and overlap in composition with phenocryst rims. Similarly, clinopyroxene Mg #s for the microlites and microphenocrysts falls within the same range as those at the rim of phenocrysts. Older samples show a much wider range in olivine composition (Fo_{58%}-84%) with the core composition of

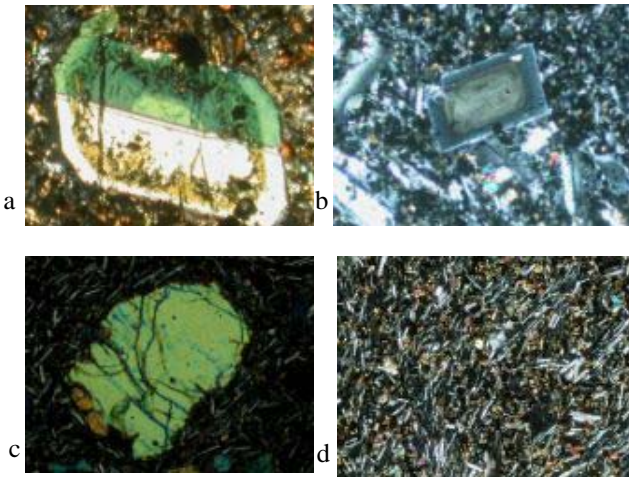


Figure 2: Photomicrographs of representative crystal textures under cross polarized light.

- An euhehedral simple twinned augite crystal (White and pale gray) showing concentric multiple zoning with resorption along a zone boundary (crystal length is 0.2 mm).
- subhedral well zoned plagioclase crystal (centre) slightly resorbed at one edge (crystal is 0.4 mm long).
- a large fractured olivine crystal (pale gray) with resorbed margins (crystal is 3.5 mm long).
- trachytic groundmass texture formed by laths of plagioclases (white streaks).

samples from one eruption being similar to the rim composition of samples from another eruption. However, clinopyroxene Mg #s show the cores of phenocrysts being less evolved (Mg # = 78 – 88) than the rims (Mg # = 78 – 85) and than the microlites for these older lavas (Mg # = 72 – 74). Plagioclase phenocryst rims overlap with the composition of microlites (Table 2). However, microphenocrysts have a similar composition to phenocryst cores as well as plagioclase inclusions in pyroxenes.

Whole Rock Geochemistry

Representative bulk rock compositions are presented in Table 3. On the TAS diagram, the older lavas plot in four major fields – basalt, basanite/trachy-basalt, hawaiiite and basaltic trachy-andesite. (Figure 3a) while 20th century lavas plot only in two fields – basanite and hawaiiite (Figure 3b). All are alkaline and are nepheline normative.

Major Element Geochemistry

The older lavas show an evolution from basalt/basanite and trachy-basalt to hawaiiite and then to basaltic trachy-andesite (BTA; mugearite). e.g., BTA have SiO₂ values >50% (50.56 – 50.96), show lowest whole-rock Mg #s (28.29 – 29.70) and highest values for differentiation index (DI; 52.32 – 54.22). Among the 20th century lavas, the 1959 samples show highest average silica content, low whole rock Mg # and the highest values of

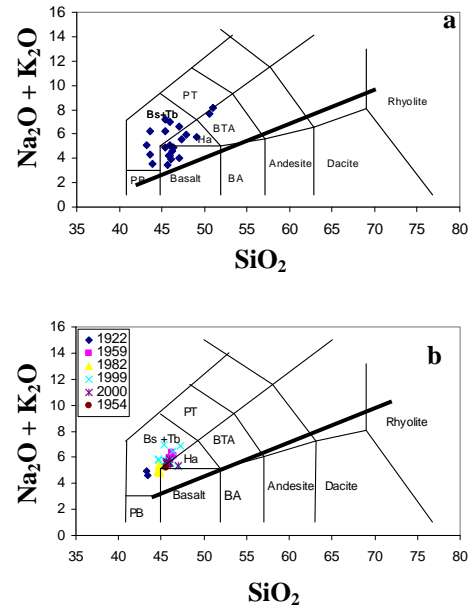


Figure 3: The Total Alkali-Silica (TAS) diagram used to classify lavas of Mt. Cameroon (after Le Bas et al. 1986). Bs: basanite; Ha: hawaiiite; PB: picobasalt; BA: basaltic-andesite; BTA: basaltic-trachy-andesite. The thick straight line separates the alkaline from the subalkaline fields (MacDonald and Katsura, 1964). a- older lavas; b-. 20th century lavas.

DI. All the lavas show a positive correlation between SiO₂, Al₂O₃, Na₂O, K₂O and P₂O₅ with DI and a negative correlation between Fe₂O₃*, MgO and CaO with DI (Figure 4).

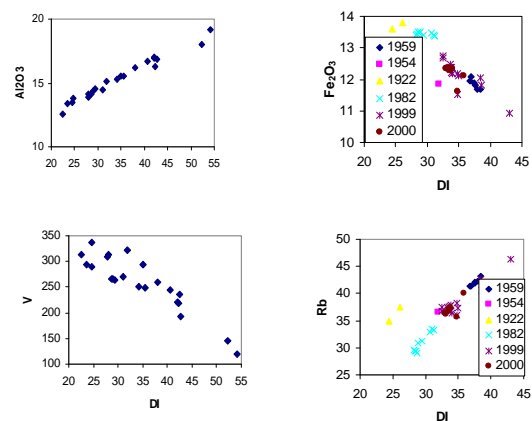


Figure 4: Representative plots of major element oxides and trace elements versus differentiation index. (The single series plots are of lavas of unknown ages).

Trace Element Geochemistry

Figure 4 show an expected negative correlation between compatible elements (Ni, Cr, V and Sc) with DI and a positive correlation between incompatible elements (Rb, Ba, Nd, Zr and Y) with DI. For the older

lavas, incompatible element values are higher and compatible element values lower for BTA and hawaiites than for basalt and basanites. Among the 20th century lavas, the 1959 lavas show higher incompatible and lower compatible element concentrations.

CONCLUSION

Magma Origin

Primitive mantle normalized spidergrams (Figure 5) show similar pattern for all the Mt. Cameroon lavas with relative depletion in K compared to similar incompatible elements. A comparison between these spidergrams, another volcano along the CVL (Mt. Manengouba) and both OIB and MORB basalts, show a great similarity in pattern between volcanoes of the CVL and OIB. Thus, the mantle source is the same for both settings. According to Dongmo et al. (2001), this mantle source is a HIMU source due to the lack of relative enrichment in incompatible elements (Rb, Ba, Th and K). This similarity to the typical OIB of Sun and McDonough (1989) provide further evidence that Mt. Cameroon lavas have not undergone strong crustal contamination, a conclusion similar to that of Nkouathio et al. (2002). A depleted mantle source for Mt. Cameroon lavas and its slightly evolved nature to OIB is confirmed by a plot of Nb/Y against Zr/Y (Figure 6) that show these lavas plotting at the extreme alkali basaltic end within the bounds of the Iceland array (Fitton et al, 1998), clearly distinct from that of the primitive mantle.

Magmatic Evolution

Variations in olivine composition between samples of different eruptions among the older lavas, in which the core composition of one remains similar to the rim composition of another has been interpreted as reflecting ingress of fresh magma batches into a chamber which forces out residual fractionated magma that continued to crystallize olivine while residing in the chamber. In this way, while the fresh batch crystallizes to form the rims of these crystals, newly crystallized olivine crystals will develop a core of same composition as the rims of these residual crystallizing crystals.

Mineral chemistry variations suggest modification of the parental magma due to simple fractional crystallization. This is emphasized by the similarity in composition of clinopyroxene and plagioclase rims and microlites, showing that the crystals were in equilibrium with the surrounding melt. Further evidence is provided by the higher anorthite content of plagioclase inclusions within pyroxene hosts, showing they must have crystallized before or at the same time as the pyroxene host and before the rest of the plagioclase population. The MgO values for the different minerals show that early fractionation of forsterite olivine and diopside clinopyroxene was followed by Fe-Ti oxides and by plagioclase. Evidence for this late plagioclase crystallization also comes from the fact that they have

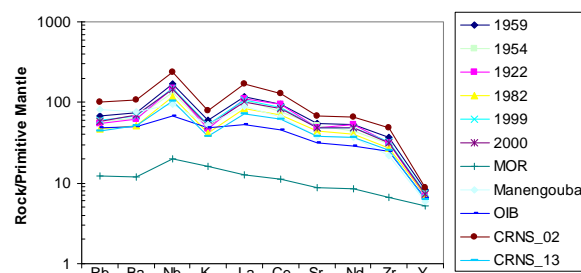


Figure 5: Trace element patterns for Mount Cameroon lavas normalised to primitive mantle values of Sun and McDonough (1989) and compared to that of a sample from Mt. Manengouba (another volcano along the CVL – values for the plot taken from Dongmo et al., 2001) and both OIB and MORB taken from 45°N in the Mid-Atlantic Ridge (values used for the plot are taken from Sun and McDonough, 1989).

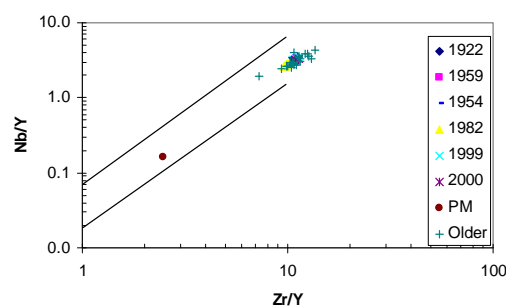


Figure 6: Nb/Y and Zr/Y variation diagram (after Fitton et al., 1998) for Mt. Cameroon volcanic rocks. The composition of the primitive mantle (PM) is shown for reference.

the smallest phenocryst sizes and lack any pure anorthite end member. This is in line with observations by Deruelle et al., 1987. Also, the occurrence of highly calcic microphenocrysts (>80 % An) in several samples suggests that plagioclase crystallization occurred at relatively shallow depths shortly before eruption.

The existence of normative nepheline indicates a less undersaturated parental magma (Njonfang and Moreau, 1996). Hence, the magma could not have been stored in large reservoirs for long periods but was probably erupted rapidly through a system of fissures, further reason for the lack of any evidence of crustal contamination and bulk assimilation in Mount Cameroon lavas.

OUTCOME

On a whole, the lower forsterite content for the older lavas, the broader plagioclase composition extending to intermediate andesine and the occurrence of basaltic trachy-andesite (BTA) provide evidence that historical eruptions involved quite evolved magmas. This supports the conclusion by Njome et al. (2008), that there is no progressive evolution of the magma with time at Mount

Cameroon. Such conclusion is a clear indication that despite the common mantle origin for all Mount Cameroon lavas, magma is supplied to the volcano in discrete batches from different chambers rather than from a single large evolving chamber as also suggested by Suh et al. (2003) and Njome et al. (2008). In this way, the different magma batches would have evolved slightly differently with subsequent mixing and mingling possibly being significant processes.

ACKNOWLEDGEMENT

This work which commenced as part of a PhD thesis was completed while N.M.S held a Lonmin-AEON postdoctoral fellowship with the Africa Earth Observatory Network (AEON), at the University of Cape Town. R.S.J. Sparks, J.G. Fitton, and the British Council are gratefully acknowledged for supervisory and financial support to the initial analytical studies in UK. N.M.S and C.E.S also acknowledge financial support from the University of Buea. Postdoctoral field studies was heavily funded by the VLIR project on "Capacity building in Geohazards monitoring in volcanically active areas of southwest Cameroon" between the University of Buea (Cameroon) and the University of Ghent (Belgium). Finally, the authors remain grateful to Lonmin Plc for supporting the postdoctoral studies of N.M.S at AEON.

REFERENCES

- Archanjo, C.J., Trindale, R.I.F., Bouchez, J.L., and Ernesto, M., 2002, Granite fabric and regional-scale strain partitioning in the Serido Belt (Borborema Province, NE Brazil): *Tectonics*, **21**(1), 1-14.
- Deruelle, B., N'ni, J. and Kambou, R., 1987, Mount Cameroon: an active volcano of the Cameroon Line: *Journal of African Earth Sciences*, **6**(2), 197 – 214.
- Deruelle, B., Bardintzeff, J-M., Cheminee, J-L., Ngounouno, I., Lissom, J., Nkoumbou, C., Etame, J., Hell, J-V., Tanyileke, G., N'ni, J., Ateba, B., Ntepe, N., Nono, A., Wandji, P., Fosso, J., and Nkouathio, D.G., 2000, Eruption simultanees de basalte alcalin et hawaiiite au mont Cameroun (28 Mars-17 Avril 1999) : *Earth and Planetary Sciences*, **331**, 525 – 531.
- Dongmo, A.K., Wandji, P., Pouclet, A., Vicat, J.P., Cheilletz, A., Nkouathio, D.G., Alexandrov, P., and Tchoua, F.M., 2001, Evolution volcanologique du mont Manengouba (Ligne du Cameroun); nouvelles donnees petrographiques, geochemiques et geochronologiques: *Compte Rendues de l'Academie de Sciences*, **333**, 155 – 162.
- Fitton, J.G., Kilburn, C.R.J., Thirlwall, M.F., and Hughes, D.J., 1983, 1982 eruption of Mount Cameroon, West Africa: *Nature*, **306**, 327 – 332.
- Fitton, J.G. and Dunlop, H.M., 1985, The Cameroon Line, West Africa, and its bearing on the origin of oceanic and continental alkali basalt: *Earth and Planetary Science Letters*, **72**, 23 – 38.
- Fitton, J.G., Saunders, A.D., Larsen, L.M., Hardarson, B.S., and Norry, M.J., 1998, Volcanic rocks from the southeast Greenland margin at 63°N: composition, petrogenesis and mantle sources: *Proceedings of the Ocean Drilling Program, Scientific Results* **152**, 331–350.
- Le Bas, M.J., Le Maitre, R.W., Streckeisen A., and Zanettin, B., 1986, Chemical classification of volcanic rocks based on the total alkali-silica diagram: *Journal of Petrology*, **27**, 745 – 750.
- MacDonald, G.A. and Katsura, T., 1964, Chemical composition of Hawaiian lavas: *Journal of Petrology*, **5**, 82 – 133.
- Ngako, V., Affaton, P., Nnange, J.M., and Njanko, T.H., 2003, Pan-African tectonic evolution in Central and Southern Cameroon: transpression and transtension during sinistral shear movements: *Journal of African Earth Sciences*, **36**, 207-214.
- Njome, M.S., Suh, C.E., Sparks, R.S.J., Ayonghe, S.N., and Fitton, J.G., 2008, The Mount Cameroon 1959 compound lava flow field: Morphology, Petrography and Geochemistry: *Swiss Journal of GeoSciences*, **101**, 85 – 98.
- Njongfang, E. and Moreau, C., 1996, The mineralogy and geochemistry of a subvolcanic alkaline complex from the Cameroon Line: the Nda Ali massif, southwest Cameroon: *Journal of African Earth Sciences*, **22**(2), 113 – 132.
- Nkouathio, D.G., Menard, J.J., Wandji, P., and Bardintzeff, J.M., 2002, The Tombel graben (West Cameroon): a recent monogenetic volcanic field of the Cameroon Line: *Journal of African Earth Sciences*, **35**, 285 – 300.
- Suh, C.E., Sparks, R.S.J., Fitton, J.G., Ayonghe, S.N., Annen, C., Nana, R., and Luckman, A., 2003, The 1999 and 2000 eruptions of Mount Cameroon: eruption behaviour and petrochemistry of lava: *Bulletin of Volcanology*, **65**, 267 – 281.
- Suh, C.E., Luhr, J.F., and Njome, M.S., 2008, Olivine-hosted glass inclusions from scoriae erupted in 1954 – 2000 at Mount Cameroon volcano, West Africa: *Journal of Volcanology and Geothermal Research*, **169**, 1 – 33.
- Sun, S-s. and McDonough, W.F., 1989, Chemical and isotopic systematics of oceanic basalts: implications for mantle composition and processes. In: Saunders, A.D. and Norry, M.L (eds), *Magmatism in the ocean basins: Geological Society of London Special Publication*, **42**, 313 – 345.

Sample No.	Points counted	Eruption year	Location (Lats & Longs)	Elevation (m)	Olivine	Clino-pyroxene	Plagioclase	Iron oxides	Groundmass	Phenocryst %
CRNS 12	2000	Unknown	04°04'48"N 09°04'59"E	480	8.2	11.5	np	0.1	80.2	19.8
CRNS 16	2000	Unknown	04°06'31"N 09°05'29"E	1098	np	9.8	0.4	0.6	89.2	10.8
CRNS 22	2000	Unknown	04°15'16"N 09°01'03"E	163	np	0.2	3.6	0.4	95.8	4.2
CRNS 19	2000	Unknown	04°01'54"N 09°11'37"E	58	1.2	np	np	np	98.8	1.2
C59U3	2000	1959	04°15'45"N 09°15'32"E	1911	2.4	10.9	4.5	0.8	81.3	18.7
C59LF	2000	1959	04°14'09"N 09°18'10"E	581	1.1	8.8	3.5	0.9	85.6	14.4
SI54/1	1700	1954	04°20'50"N 09°17'38"E	4000	9.1	17	16.3	3.2	54.4	45.6
SI82/1	1500	1982	04°08'23"N 09°06'27"E	1958	0.5	0.7	0.8	np	98	2
SI99/1	2000	1999	04°06'11"N 09°07'04"E	1545	7.8	5.7	4.8	1.1	80.6	19.4
SI99/3	2500	1999	04°09'18"N 09°08'17"E	2734	7.8	8.9	5.8	2	75.7	24.5
SI2000/1	1800	2000	04°12'40"N 09°10'37"E	3880	5.3	10.1	1.8	0.9	81.9	18.1
SI2000/3	2000	2000	04°12'38"N 09°10'37"E	3730	6.1	8.7	2.9	1.8	80.5	19.5

Table 1: Modal composition of representative Mt. Cameroon lava samples (Vol %, vesicle free) determined by counting more than 1500 points. (np = not present).

Olivine															
Sample No./Year	CRNS 08/Older			CRNS 12/Older			C59LE/1959			1999			2000		
Analysis No.	1	2	3	4	5	6	4	5	2	2	1	5	9	10	11
Region	r	c	m	r	c	m	r	c	m	r	c	m	r	c	m
Fo%	75.25	77.25	57.72	78.94	78.67	67.88	72.9	80.5	69.2	69.6	83.2	68	76.9	83.6	67.8
Clinopyroxene															
Sample No./Year	CRNS 08/Older			CRNS 12/Older			C59LE/1959			1999			2000		
Analysis No.	1	2	3	4	5	6	5	8	1	2	1	5	7	6	10
Region	r	c	m	r	c	m	r	c	m	r	c	m	r	c	m
Mg#	78.52	86.87	72.77	84.96	88.02	74.20	78.44	80.82	76.63	75	76	75	70	83	65
Plagioclase															
Sample No./Year	CRNS 07/Older			CRNS 26/Older			C59LE/1959			1999					
Analysis No.	1	2	3	4	5	6	4	8	1	4	1	5	1	2	3
Region	r	c	m	r	c	m	r	c	m	r	c	m	r	c	m
An %	70.92	82.57	59.39	55.42	73.73	57.67	62.37	80.17	54.92	50.7	84.4	48.7	70.92	82.57	59.39

Table 2: Representative microprobe analyses of different crystal phases in Mount Cameroon lava samples. (r = rim; c = core; m = microlite). (Data for 1959 are taken from Njome et al., 2008; while that for 1999 & 2000 are from Suh et al., 2003)

Eruption Year	Unknown	Unknown	Unknown	Unknown	1959	1954	1922	1982	1999	2000
Sample No.	CRNS_09	CRNS_12	CRNS_07	CRNS_08	C59LF	SI54/1	C25	C194	BA3	SM7
Major Element concentrations expressed in weight percent										
SiO ₂	43.84	43.62	46.19	45.68	46.21	45.63	43.47	44.81	45.79	45.83
TiO ₂	3.87	3.41	2.76	3.08	3.25	3.12	3.08	3.40	3.09	3.12
Al ₂ O ₃	12.54	13.81	14.42	13.36	15.76	15.01	12.05	15.13	15.04	15.21
Fe ₂ O ₃	14.22	13.95	12.41	13.34	12.08	11.86	13.60	13.48	12.34	12.36
MnO	0.24	0.21	0.21	0.19	0.22	0.2	0.21	0.20	0.21	0.20
MgO	8.33	7.3	7.21	7.82	5.56	7.21	10.64	6.01	7.05	6.76
CaO	11.99	12.18	11.5	12.2	10.27	11.01	11.64	11.92	10.53	10.52
Na ₂ O	2.52	3.06	3.35	2.41	4.27	3.77	3.19	3.62	3.99	4.01
K ₂ O	1.05	1.25	1.23	1.03	1.73	1.45	1.40	1.28	1.54	1.54
P ₂ O ₅	0.56	0.67	0.45	0.43	0.81	0.65	0.73	0.55	0.67	0.68
LOI	0.24	-0.37	-0.05	-0.07	-0.50	-0.34	n.d	n.d	-0.60	-0.51
Total	99.39	99.09	99.68	99.47	99.65	99.57	100.00	100.39	99.65	99.74
Mg#	39.43	36.77	39.23	39.44	33.84	40.32	46.52	33.14	38.83	37.82
CIPW Norms expressed in weight percent										
Or	6.21	7.39	7.27	6.09	10.22	8.57	8.27	7.56	9.10	9.10
Ab	10.41	7.25	13.88	13.98	15.63	13.11	3.24	9.82	13.21	13.70
An	19.8	20.25	20.68	22.59	18.73	19.75	14.43	21.25	18.58	18.95
Ne	5.91	10.1	7.84	3.47	11.10	10.18	12.87	11.27	11.14	10.96
Di	29.57	29.53	27.52	28.88	22.29	25.06	31.42	28.43	24.08	23.71
Ol	16.55	14.89	14.47	15.75	12.38	13.58	20.27	12.37	14.94	14.51
Ilm	7.35	6.48	5.24	5.85	6.17	5.93	5.85	6.46	5.87	5.93
Mt	2.06	2.03	1.8	1.93	1.75	1.83	1.97	1.96	1.78	1.80
Ap	1.3	1.55	1.04	1	1.88	1.51	1.69	1.27	1.55	1.58
DI	22.53	24.74	28.99	23.54	36.95	31.86	24.38	28.65	33.45	33.76
Trace element concentrations expressed in ppm										
Rb	27.28	29.56	31.84	23.02	41.45	36.6	35.01	28.96	36.98	37.18
Ba	402.43	382.39	433.19	365.03	518.72	450	436.98	369.73	481.66	489.63
Nb	77.34	90.72	90.33	69.9	117.30	96.2	106.59	82.69	102.39	103.54
La	49.81	57.91	63.47	62.15	76.84	73.8	76.56	58.50	67.76	68.98
Ce	117.28	129.57	132.94	111.92	163.28	137.1	166.94	124.29	147.84	149.90
Sr	853.6	914.93	903.22	788.6	1131.41	1077	1014.17	901.87	1019.14	1029.92
Nd	59.66	63.03	60.25	59.85	74.14	59.2	72.38	56.80	64.60	65.17
Zn	106.87	111.25	104.22	97.11	105.59	113	118.73	119.77	108.89	108.68
Cu	82.5	73.01	89.56	117.72	62.21	76	68.86	107.14	73.09	74.20
Sc	25.8	23.6	25.3	28.2	15.90	26	31.21	25.89	20.59	20.81
Zr	320.45	319.47	318.21	263.88	395.99	339	352.38	300.39	354.79	357.42
Y	30.7	30.9	31.1	36.16	36.16	33.35	31.51	31.00	33.18	33.08
Ni	126.98	89.4	87.63	112.91	46.31	99	181.14	58.43	85.59	80.97
Cr	258.57	187.16	181.43	235.07	76.07	213	466.28	57.52	141.59	136.32
V	312.7	337.3	265.8	293.9	248.30	295	273.90	317.70	255.85	251.57

Table 3: Representative whole-rock XRF major and trace element compositions including CIPW norms for Mount Cameroon older lavas compared with data for 1954 (Suh et al., 2008), 1959 (Njome et al., 2008), 1922 , 1982 (Fitton et al., 1983) and 1999, 2000 (Suh et al., 2003). DI, is differentiation index of Thornton and Tuttle (1960) defined as: $DI = CIPW \text{ normative } Qz + Or + Ab + Ne$.